Supplement of Geosci. Model Dev., 13, 4323–4353, 2020
https://doi.org/10.5194/gmd-13-4323-2020-supplement

Geoscientific Model Development
Open Access
EGU

Supplement of

The urban dispersion model EPISODE v10.0 – Part 1: An Eulerian and sub-grid-scale air quality model and its application in Nordic winter conditions

Paul D. Hamer et al.

Correspondence to: Paul D. Hamer (paul.hamer@nilu.no)

S1. Standard K (z)-method

The standard K (z) -method is the default method for calculation of the vertical eddy diffusivity in the EPISODE dispersion model. The standard method is based upon the description in Byun et al. (1999). The standard K (z)-method uses a constant background diffusivity of $K_0^{(z)}$ = 0.01 m^2 s^{-1}.

The stability regime affecting the K (z)-method is defined with a non-dimensional number z/L, where z is the height above the ground and L is the Monin-Obukhov length. In accordance with K-theory it is assumed that chemical species have non-dimensional profile characteristics similar to potential temperature, θ, such that $K^{(z)}$ equals the eddy diffusivity of the heat flux, K_H.

The non-dimensional profile functions of the vertical gradient of potential temperature, Θ, are expressed as:

$$\phi_H = \mathrm{Pr}_0\left(1 + \beta_H \frac{z}{L}\right) \quad \text{for moderately stable } \left(1 \geq \frac{z}{L} > 0\right) \quad \text{(S1.1a)}$$

$$\phi_H = \left(1 - \gamma_H \frac{z}{L}\right) \quad \text{for unstable and neutral } \left(\frac{z}{L} \leq 0\right) \quad \text{(S1.1b)}$$

Where Pr_0 is the Prandtl number for neutral stability and β_H and γ_H are coefficients of the profile functions determined through field experiments. For very stable conditions $\left(\frac{z}{L} > 1\right)$ the expression suggested by Holtslag et al. (1990) is used to extend the applicability of the surface similarity:

$$\phi_H = \mathrm{Pr}_0\left(\beta_H + \frac{z}{L}\right) \quad \text{(S1.1c)}$$

Within the planetary boundary layer (PBL), vertical eddy diffusivity is parameterized with:

$$K_*^{(z)} = \frac{\kappa u_* z(1 - z/h_{mix})^{3/2}}{\phi_H(z/L)} \quad \text{for } \frac{z}{L} > 0 \text{ (stable)} \quad \text{(S1.2a)}$$

$$K_*^{(z)} = \kappa w_* z(1 - z/h_{mix}) \quad \text{for } \frac{z}{L} \leq 0 \text{ (unstable and neutral),} \quad \text{(S1.2b)}$$

where κ = 0.41 is the Von Kármán constant, u_* is the friction velocity (m s^{-1}) and w_* is the convective velocity (m s^{-1}), h_{mix} is the height of the PBL (mixing height) above the urban area.

For each vertical model layer, the eddy diffusivity is calculated iteratively within 5 sub-layers. The vertical eddy diffusivity of the respective layer is obtained as vertical average of the sub-layer diffusivities.

S2. Photo-stationary steady state

The photo-stationary state (PSS) is an analytical mathematical solution corresponding to reaction (R4) in Section 2.2.1 of part 1 of this paper. This reaction describes an equilibrium between the production of NO_2 from reaction (R1) and the loss of NO_2 from reactions (R2) and (R3). The resulting equilibrium level of NO_2 can thus be found by solving the following equation

$$\frac{dNO_2}{dt} = k_1 NO \cdot O_3 - k_2 NO_2 = 0, \tag{S2.1}$$

where $k_1 = k_{(O3+NO)}$ is the reaction coefficient between NO and O_3 in the production of NO_2, and $k_2 = jNO_2$ is the reaction coefficient of photolysis in the loss of NO_2 (Simpson et al., 1993). These reaction coefficients are defined as follows

$$k_1 = 1.4 \cdot 10^{-12} \exp\left(-1310 / T_{air}\right) \tag{S2.2a}$$

and

$$k_2 = \begin{cases} 1.45 \cdot 10^{-2} \left(1 - 0.5CC\right) \exp\left(-0.4/\sin\varphi\right) & \varphi > 0 \\ 0 & \varphi \le 0 \end{cases}, \tag{S2.2b}$$

where T_{air} is the air temperature in degrees Kelvin, CC is the cloud cover as a fraction of 1, and φ is the Sun's height above the horizon in degrees.

Replacing NO with $NO_x - NO_2$ and O_3 with $O_x - NO_2$, Eq. (S2.1) can alternatively be written

$$k_1 \left(NO_x - NO_2\right)\left(O_x - NO_2\right) - k_2 NO_2 = 0, \tag{S2.3}$$

where $NO_x = NO + NO_2$ and $O_x = NO_2 + O_3$ are inert species whose concentration levels are constant regarding the production and loss reactions (R1) - (R3). Thus, given the levels of NO_x and O_x in a volume of air, solving Eq. (S2.3) gives the level of NO_2 corresponding to the PSS. The resulting levels of NO and O_3 are then found as $NO = NO_x - NO_2$ and $O_3 = O_x - NO_2$.

Re-ordering Eq. (S.2.3) it can be written

$$aNO_2^2 + bNO_2 + c = 0\,, \qquad \text{(S2.4)}$$

with $a = k_1$, $b = -k_1\left(NO_x + O_x\right) - k_2$ and $c = k_1 NO_x O_x$. Thus, the PSS solution is found by solving this second-degree equation in NO_2 and using the root which is smaller than min(NO_x, O_x). From Eq. (S2.3) it is easily seen that such a root can always be uniquely found since k_1 and k_2 are non-negative.

Applying Eq. (S2.4), concentrations of NO_2, NO and O_3, and NO_x and O_x, are converted to molecules·cm^{-3} in order to define the coefficients b and c. Then Eq. (S2.4) is solved for NO_2 in this unit before being transformed back to the original unit, e.g. µgm^{-3}.

The PSS solution for NO_2 is applied in EPISODE for each grid cell of the Eulerian model and at each receptor point for the sub-grid scale model. This is done in an instantaneous way during every dynamical time step without considering the time it takes to reach the equilibrium. Thus, the model first calculates the levels of NO_x and O_x for each grid cell and receptor point during each time step, and then it solves Eq. (S2.4) to find the PSS levels of NO_2, NO and O_3 at each grid cell and receptor.

S3. Injection height scheme for point sources

The injection height of emissions from (elevated) point sources into the vertical layers of the EPISODE model is calculated based on a detailed plume rise algorithm. Plume rise due to momentum or buoyancy is considered using the plume rise equations originally presented by Briggs (1969, 1971 and 1975) and takes into account different boundary layer (BL) stability conditions as characterized by the inverse Monin-Obukhov length (L^{-1}). The physical stack height of the point source is modified according to Briggs (1974) to account for situations with stack downwash. Final plume rise is calculated considering the effects of (1) the adjacent building due to building-induced disturbances of the flow (Briggs, 1974); (2) penetration through an elevated stable layer; and (3) topography. Input parameters for the point source emission module include pollutant emission rates, stack height, diameter, exhaust gas temperature and exit velocity as well as height and width of the building adjacent to the stack. The input parameters can be specified for each point source by the model user.

Stack downwash

The stack downwash process modifies the physical height of the chimney to estimate an effective stack height (Briggs, 1974). An effluent emitted vertically from a stack can rise due to its momentum, or be brought downward by the low pressure in the wake of the stack. What happens in a given situation depends on the ratio of the exit gas velocity to the wind velocity.

The physical stack height, h_s is modified according to Briggs (1974):

$$h'_s = h_s + 2\left(\frac{V_s}{u} - 1.5\right) \cdot D \qquad \text{for } w_s < 1.5u \qquad \text{(S.3.1a)}$$

$$h'_s = h_s \qquad \text{for } w_s \geq 1.5u \qquad \text{(S.3.1b)}$$

where V_s is the exit gas velocity, u is the wind speed at plume height, and D is the inside stack-top diameter. The modified stack height, h'_s, is further used to calculate effective plume height, H_{eff}.

Buoyancy driven and momentum driven plume rise

Buoyancy driven plume rise will affect the final plume height in different ways according the boundary layer stability conditions, and therefore there are different parameterisations for either unstable and neutral conditions, or stable conditions. A decision flow diagram of the buoyancy and momentum driven plume rise is depicted in Figure S3.1.

The wind speed at plume height, u, is calculated using a logarithmic wind speed profile corrected by the stability function for momentum based on Holtslag and de Bruin (1988).

Regardless of the atmospheric stability, the plume rise algorithm at first calculates the *neutral-unstable momentum rise*, Δh_{nm}, as follows:

$$\Delta h_{nm} = 3DV_s u^{-1} \qquad \text{(S3.2)}$$

Equation Eq. (S3.2) is most adequate when V_s/u is greater than four. Since momentum rise occurs quite close to the point of release, the distance to final rise, x_f, is set equal to zero.

The boundary flux parameter, F (m^4 s^{-3}), is needed for calculation of the buoyant plume rise, Δh_b, defined by

$$F = (gV_s D^2 \Delta T)/(4T_s) \ , \qquad \text{(S3.3)}$$

where $\Delta T = T_s - T_a$; T_s is the stack gas temperature (K) and T_a is the ambient air temperature (K).

The distance to final plume rise, x_f (km), is the distance at which atmospheric turbulence begins to dominate entrainment into the plume. The expression of x_f depends on the value of the boundary flux parameter and is given by:

$$x_f = 0.049 \cdot F^{5/8} \qquad \text{for } F < 55 \qquad \text{(S.3.4a)}$$

$$x_f = 0.119 \cdot F^{2/5} \qquad \text{for } F \geq 55 \qquad \text{(S.3.4b)}$$

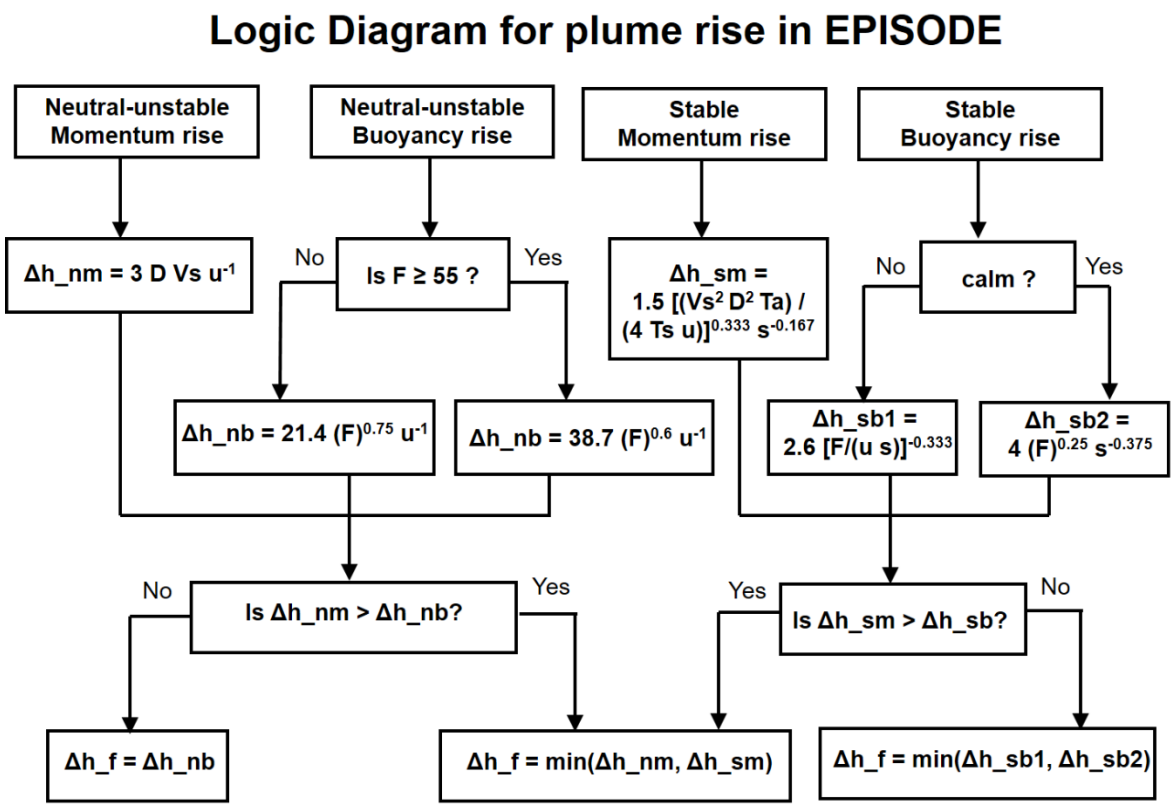

Figure S3.1: Logic diagram of the plume rise algorithm for buoyancy and momentum driven plume rise for different atmospheric stability conditions. In the diagram, F is the buoyancy factor ($m^4\ s^{-3}$), V_s is stack exit velocity ($m\ s^{-1}$), D is stack diameter (m), T_a is ambient temperature (K), T_s is exhaust gas temperature (K), u is wind speed at actual stack height ($m\ s^{-1}$), and s is the stability parameter (s^{-2}). Diagram after Karl et al. (2014).

The *neutral-unstable buoyancy rise*, Δh_{nb}, is determined depending on F, as follows:

$$\Delta h_{nb} = 21.425 \cdot F^{3/4} \cdot u^{-1} \qquad \text{for } F < 55 \qquad \text{(S.3.5a)}$$

$$\Delta h_{nb} = 38.71 \cdot F^{3/5} \cdot u^{-1} \qquad \text{for } F \geq 55 \qquad \text{(S.3.5b)}$$

If the neutral-unstable momentum rise, calculated from Eq. (S3.2), is larger than the neutral-unstable buoyancy rise calculated here, momentum rise applies and the distance to final rise is set equal to zero.

For stable conditions, the stability parameter, s, is calculated from:

$$s = g(\partial\theta/\partial z)/T_a. \quad \text{(S3.6)}$$

The vertical gradient of the potential temperature, $\partial\theta/\partial z$, is approximated by 0.02 K m^{-1} for the slight stable case and as 0.035 K m^{-1} for the stable case. When the stack gas temperature is less than the ambient air temperature, it is assumed that the plume rise is dominated by momentum. The *stable momentum rise*, Δh_{sm}, is calculated by the equation:

$$\Delta h_{sm} = 1.5 \cdot [(V_s^2 D^2 T_a)/(4 T_s u)]^{1/3} \cdot s^{-1/6} \quad \text{(S3.7)}$$

The value of Δh_{sm}, is compared to the value of neutral-unstable momentum rise, Δh_{nm}, and the lower of the two values is used as the resulting plume rise.

For situations where $T_s \geq T_a$, buoyancy is assumed to be dominant. For such conditions, the distance to final rise is determined by:

$$x_f = 0.0020715 \cdot u \cdot s^{-1/2}, \quad \text{(S3.8)}$$

and the *stable buoyancy rise*, Δh_{sb}, is expressed as:

$$\Delta h_{sb} = 2.6 \cdot [F/(u \cdot s)]^{1/3} \quad \text{(S3.9)}$$

For calm conditions the stable buoyancy rise is in addition evaluated as:

$$\Delta h_{sb} = 4 \cdot F^{1/4} \cdot s^{-3/8}, \quad \text{(S3.10)}$$

and the lower of the values obtained from equations Eq. (S3.9) and Eq. (S3.10) is taken as the final estimate of the buoyant plume rise.

If the stable momentum rise is higher than the stable buoyancy rise, momentum rise applies and then the distance to final rise is set equal to zero.

The final injection height is subsequently calculated by taking into account the effects of the adjacent buildings (considering their height and width) on building-induced disturbances of the plume flow, plume penetration through elevated stable layers, and topography.

Building effects

The estimation of the effective height of emission due to building-induced disturbances to the flow follows the procedure outline by Briggs (1974). An intermediate plume height, h', is calculated based on the momentum rise, Δh_m (from either Eq. (S3.2) or Eq. (S3.7)):

$$h' = h_s + \Delta h_m \qquad \text{(S3.11)}$$

The intermediate plume height is set to h_s' if stack downwash occurs (Eq. (S3.1)).

Next, the relation of the intermediate plume height to the building dimensions, i.e. building height H_B and building width, W_B, of the building close to the stack is evaluated. Let the building length be $L_B = \min(H_B, W_B)$, then two cases can be distinguised:

1. If $h' > H_B + 1.5L_B$: the plume is above the region of building influence. The building effect does not need to be considered.
2. If $h' < H_B$ or if $H_B < h' < H_B + 1.5L_B$: the plume may remain aloft or may be entrained into the wake cavity and become essentially a ground level source. The building effect needs to be considered.

In the second case, the following case division is done for calculation of the building-influenced plume height, h_{bd}:

$$h_{bd} = h' - 1.5L_B \qquad \text{for } h' < H_B \qquad \text{(S.3.12a)}$$

$$h_{bd} = 2h' - (H_B + 1.5L_B) \qquad \text{for } H_B < h' < H_B + 1.5L_B \qquad \text{(S.3.12b)}$$

Further, if h_{bd} is greater than $0.5L_B$, the plume remains elevated and concentrations can be calculated by using the standard formulas with modified stack height equal to h_{bd}. The plume penetration is checked next.

However, if h_{bd} is less than $0.5L_B$, the plume is influenced by the buildings. In this case an additional dispersion factor is combined with the standard dilution factor (Briggs, 1971):

$$\sigma_y = \sqrt{\sigma_y^2 + \frac{cA}{\pi}}\ , \qquad \text{(S3.13)}$$

and

$$\sigma_z = \sqrt{\sigma_z^2 + \frac{cA}{\pi}}\ , \qquad \text{(S3.14)}$$

where $c = 1.0$ and $A = H_B \cdot W_B$.

Plume penetration

A buoyant plume rising into a well-mixed layer capped by stable air may partially or completely penetrate the elevated stable layer. To compute ground level concentrations for this situation, the fraction of the plume that penetrates the stable layer is first estimated and then the emission rate, q_p, and effective plume height, H_{eff}, for the material remaining within the mixed layer are modified. First, the fraction P of the plume that penetrates the elevated stable layer is estimated (Weil and Brower, 1984):

$P = 0$	if $\frac{z_i'}{\Delta h} \geq 1.5$	(no penetration)	(S.3.15a)
$P = 1$	if $\frac{z_i'}{\Delta h} \leq 0.5$	(total penetration)	(S.3.15b)
$P = 1$	if $0.5 < \frac{z_i'}{\Delta h} < 1.5$	(partial penetration),	(S.3.15b)

where Δh is the predicted plume rise due to buoyancy and/or momentum and $z_i' = z_i - h_s$ with z_i being the height of the stable layer aloft. The plume material remaining within the mixed layer is assumed to contribute to ground level concentrations. The modified source strength, q is then:

$$q = q_s \cdot (1 - P), \qquad \text{(S3.16)}$$

where q_s is the emission rate on top of the stack.

To modify the effective plume height for plumes that are trapped within the mixed layer, it is assumed that the plume rise due to penetration, Δh_p, varies linearly between $0.62 \cdot z_i'$ (for no penetration) and z_i' for total penetration, and thus for partial penetration is:

$$\Delta h_p = (0.62 + 0.38 \cdot P) \cdot z_i' \qquad \text{(S3.17)}$$

The modified plume height, h_m, is the lowest value of the height in the unlimited atmosphere obtained from the evaluation of the building effect and of the penetration effect:

$$h_m = min(h_{bd}, h_p) \qquad \text{with } h_p = h_s' + \Delta h_p \qquad \text{(S3.17)}$$

Topography effects

The effect of elevated terrain, for instance a hill in proximity of the point source, on the ground level concentrations is considered by reducing h_m, from Eq. S(3.17), giving the effective plume height, H_{eff}:

$$H_{eff} = h_m - \Delta H_t, \qquad with\ \Delta H_t = k \cdot h_t, \qquad \text{(S3.18)}$$

Where h_t is the height of terrain above stack level and k is a terrain factor ($0 < k < 1$) depending upon steepness, distance from source, stability and other parameters. The method used to evaluate the effect of a hill on a source as function of distance from the point sources is given in Table S3.1. The effect of elevated terrain on the ground level concentrations decreases with increasing distance from the source.

Table S3.1: Topography effect on plume rise. Terrain factor k to evaluate the effect of a hill on a point source with stack height h_s.

Distance from source (x)	Terrain factor k
$0 < x \leq 5h_s$	0.7
$5h_s < x \leq 10h_s$	0.5
$10h_s < x \leq 20h_s$	0.3
$20h_s < x \leq 30h_s$	0.1
$30h_s < x$	0.0

S4. Line source Gaussian dispersion (HIWAY-2)

The HIWAY-2 model (Highway Air Pollution Model 2; Petersen, 1980) developed by US EPA is applicable for any wind direction, street orientation, and receptor location at distances tens to hundreds of meters downwind of the line source, given that the terrain is relatively uncomplicated. HIWAY-2 computes the concentration of a pollutant by numerically integrating the Gaussian plume point source equation over a finite length of the road. Each street lane (or lane segment) with vehicle traffic is simulated as a straight, continuous, finite length, line source with a uniform emission rate. The emission intensity on each of the lanes is assumed to be uniform along the line source. Pollutant concentrations caused by vehicle traffic are found by interpretation of the line source as a finite sum of simple Gaussian point-source plumes, and the total line source contribution is then derived by numerical integration (i.e. summation) over the length of the line source, thinking of the line source as a line-of-points.

The concentration contribution $C_{line,s}$ at the receptor point r^* from traffic emissions is found by integrating the concentration contributions from each of the infinitesimal point sources along the line source s, according to:

$$C_{line,s} = \left(\frac{Q_s}{\mathrm{u}}\right) \cdot \int_0^L f ds \qquad \text{(S.4.1)}$$

where Q_s (in g m^{-1} s^{-1}) is the emission intensity from the line source, L is the source length (in m), ds is an infinitesimal line segment (in m), and f is the point source dispersion function (in m^{-2}). Each of the point sources is placed in the middle of the lane, m_l, with distance of a half lane width, $W_l/2$, from the middle of the street.

The integral in Eq. (S4.1) is approximated by use of Richardson extrapolation of the trapezoidal rule. Estimates are made dividing the line source into a number of intervals equal to 3, 6, …, $3 \cdot (2)^9$.

Calculations are successively repeated for each partition class until the concentration estimates converge to within 2 percent of the previous estimate (Petersen, 1980).

The sub-grid model for line sources distinguishes between four classes of atmospheric stability by evaluating the temperature difference between a lower height (z_1) and an upper height (z_2) in the two lowest model layers, $\Delta T = (z_2 - z_1)dT/dz$. Table S4.1 shows how the stability classes are related to the Pasquill-Gifford (P-G) classes.

For stable conditions or when the diffusion in the vertical is unlimited, the ordinary point source Gaussian dispersion function is used in Eq. (S4.1), given by:

$$f = \frac{1}{2\pi \cdot \sigma_y \cdot \sigma_z} \cdot \exp\left[-\frac{y_r^2}{2\sigma_y^2}\right] \cdot \left\{\exp\left[-\frac{(z_r - H_{tr})^2}{2\sigma_z^2}\right] + \exp\left[-\frac{(z_r + H_{tr})^2}{2\sigma_z^2}\right]\right\} \quad \text{(S4.2)}$$

where H_{tr} is effective emission height (m) from traffic, assumed to be zero; z_r is the receptor height above ground (m), set to 2 m. The calculation of the crosswind and vertical dispersion parameters σ_y and σ_z is described below.

For unstable or neutral conditions, given that σ_z is larger than 1.6 times the mixing layer height, h_{mix}, the concentration distribution below the mixing layer is considered to be uniform with height, regardless of either source or receptor height:

$$f = \frac{1}{\sqrt{2\pi} \cdot \sigma_y \cdot h_{mix}} \cdot \exp\left[-\frac{y^2}{2\sigma_y^2}\right] \quad \text{(S4.3)}$$

Table S4.1: Atmospheric stability classes in the sub-grid model components.

Stability class	Name	Temperature difference ΔT between 10 m and 25 m	Mapping to P-G class	Line-source parameterization of ambient turbulence			
				a	b	c	d
1	Unstable	ΔT < -0.5°	A, B, C	110.62	0.932	18.333	1.8096
2	Neutral	-0.5° < ΔT < 0.0°	D	86.49	0.923	14.333	1.7706
3	Moderately stable	0.0° < ΔT < 0.5°	E	61.14	0.915	12.5	1.0857
4	Stable	ΔT > 0.5°	F	61.14	0.915	12.5	1.0857

For all other unstable or neutral conditions, multiple reflections at the ground are taken into account, and the following Gaussian dispersion function is used:

$$f = \frac{1}{2\pi\cdot\sigma_y\cdot\sigma_z}\cdot\exp\left[-\frac{y_r^2}{2\sigma_y^2}\right]\cdot\left\{\exp\left[-\frac{(z_r-H_{tr})^2}{2\sigma_z^2}\right]+\exp\left[-\frac{(z_r+H_{tr})^2}{2\sigma_z^2}\right]\right.$$
$$+\sum_{n=1}^{\infty}\left(\exp\left[-\frac{1}{2}\left(\frac{z-H_{tr}-2n\cdot h_{mix}}{\sigma_z}\right)^2\right]+\exp\left[-\frac{1}{2}\left(\frac{z+H_{tr}-2n\cdot h_{mix}}{\sigma_z}\right)^2\right]\right.$$
$$\left.\left.+\exp\left[-\frac{1}{2}\left(\frac{z-H_{tr}+2n\cdot h_{mix}}{\sigma_z}\right)^2\right]+\exp\left[-\frac{1}{2}\left(\frac{z+H_{tr}+2n\cdot h_{mix}}{\sigma_z}\right)^2\right]\right)\right\} \quad \text{(S4.4)}$$

The infinite sum series in Eq. (S4.4) converges rapidly, more than five summations ($n = 5$) of the four sum terms are seldom required (Petersen, 1980). In Equations (S4.2) to (S4.4) the dispersion parameters are evaluated for the given atmospheric stability class and downwind distance x.

In the sub-grid line source model component, the dispersion parameters are generally defined as:

$$\sigma_y = \sqrt{\sigma_{ya}^2 + \sigma_{y0}^2} \quad \text{(S.4.5a)}$$

$$\sigma_z = \sqrt{\sigma_{za}^2 + \sigma_{z0}^2} \quad \text{(S4.5b)}$$

where σ_{ya} is the crosswind dispersion and σ_{za} is the vertical dispersion, respectively, resulting from ambient turbulence, σ_{y0} is the initial crosswind dispersion and σ_{z0} is the initial vertical dispersion.

In the modified version of HIWAY-2 used in EPISODE, the initial spread of the plume from traffic due to vehicle induced turbulence depends on the wind speed (Slørdal et al., 2003):

$$\begin{cases} \sigma_{y0} = 3 & ;\ \mathrm{u} > 3.0\ ms^{-1} \\ \sigma_{y0} = 10 & ;\ \mathrm{u} < 1.0\ ms^{-1} \\ \sigma_{y0} = 10 - \left(7 \cdot \frac{u-1.0}{2.0}\right) & ;\ 1.0\ ms^{-1} \leq \mathrm{u} \leq 3.0\ ms^{-1} \end{cases} \quad \text{(S4.6a)}$$

$$\begin{cases} \sigma_{z0} = 1.5 & ;\ \mathrm{u} > 3.0\ ms^{-1} \\ \sigma_{z0} = 5 & ;\ \mathrm{u} < 1.0\ ms^{-1} \\ \sigma_{z0} = 5 - \left(3.5 \cdot \frac{u-1.0}{2.0}\right) & ;\ 1.0\ ms^{-1} \leq \mathrm{u} \leq 3.0\ ms^{-1} \end{cases} \quad \text{(S4.6b)}$$

The crosswind dispersion due to ambient turbulence is given by (Petersen, 1980):

$$\sigma_{ya} = 1000 \cdot x \cdot \frac{\sin\theta_p}{2.15 \cdot \cos\theta_p} \quad \text{(S4.7)}$$

where x is the downwind distance (in km) and θ_p is the half angle of the crosswind plume spreading, given by:

$$\theta_p = \mathrm{c} - \mathrm{d} \cdot \ln\left(\frac{x}{x_0}\right) \quad \text{(S4.8)}$$

In Eq. (S4.8), c and d are constants depending on stability and x_0 is the normalizing distance (here 1 km is used). The vertical dispersion due to ambient turbulence is given by (Petersen, 1980):

$$\sigma_{za} = \mathrm{a} \cdot x^{\mathrm{b}} \qquad \text{(S4.9)}$$

The empirical constants a and b depend on the stability. Values of a, b, c, and d are tabulated in Table S4.1. Sufficiently far downwind the atmospheric dispersion process dominates. At 300 m downwind the above described dispersion curves are merged into the P-G dispersion curves.

At present deposition (dry or wet) is not explicitly included as a sink term in the line source model component.

S5. Plume segments (SEGPLU)

The Gaussian segmented plume model SEGPLU (Walker and Grønskei, 1992) computes and keeps record of the subsequent positions of the plume segments and the pollutant concentration within each of the plume segments released from a point source. SEGPLU treats the emission from individual point sources as a temporal sequence of instantaneous releases of a specified pollutant mass. The finite length plume segments are emitted at discrete time intervals ΔT given by $\Delta T = 3600(s)/2n$, where n is an integer value, which depends on the meteorological conditions and becomes larger as the wind speed increases. The segments are redirected at every grid point and every simulation hour according to changes of the wind flow field. The subsequent position of plume segments and pollutant concentration within each of the plume segments is then calculated.

The initial horizontal position of the plume segment corresponds to the (x, y)-coordinates of the point source and the initial vertical position is estimated from plume rise formulas, where the plume rise is determined by stack height, stack exit velocity of the emitted pollutant and buoyancy of the effluent.

The length of the plume segment is prescribed as $L_{seg} = u \cdot \Delta t$ and the direction of the plume is set equal to the wind direction at the point source. The mass of a pollutant $M_{seg,i}$ in the plume segment depends on the point source emission rate $Q_{p,i}$, in the form $M_{seg,i} = Q_{p,i} \cdot \Delta t$. While the plume segments are transported by horizontal advection, the new position of the plume segment (X_{seg}, Y_{seg}) as function of the travel time t (time since release) is calculated as:

$$X_{seg}(t + \Delta t) = X_{seg}(t) + \mathrm{u}\Delta t \qquad \text{and}$$
$$Y_{seg}(t + \Delta t) = Y_{seg}(t) + \mathrm{v}\Delta t \qquad \text{(S5.1)}$$

The cross-wind dispersion of each plume segment is calculated according to (Irwin, 1983):

$$\sigma_y(t) = \sigma_v \cdot t \cdot \left(1/\left(1 + 0.9\sqrt{t/1000}\right)\right) \quad \text{(S5.2)}$$

The vertical dispersion of the plume segments is calculated according to the expression by Venkatram et al. (1984):

$$\sigma_z(t) = \sigma_w \cdot t \cdot \sqrt{1 + \frac{t}{2T_L}} \quad \text{(S5.3)}$$

The standard deviation of the horizontal wind fluctuations, σ_y, and the vertical wind fluctuations, σ_w, are calculated using the profile method (as described in Slørdal et al. (2003); section 2.1 therein). The Lagrangian timescale T_L is defined as:

$$T_L = \frac{\lambda}{\sigma_w} \quad \text{(S5.4)}$$

The dispersion length λ is specified as $\lambda^{-1} = \lambda_s^{-1} + \lambda_n^{-1}$ with:

$$\lambda_s = \frac{\gamma^2 \sigma_w}{N} \quad \text{and} \quad \lambda_n = \alpha \cdot z \quad \text{(S5.5)}$$

Where γ and α are empirical coefficients with values of 0.52 and 0.36, respectively, and N is the Brunt-Vaisala frequency, defined as:

$$N = \sqrt{\frac{\mathrm{g}}{T}\frac{d\theta}{dz}} \quad \text{(S5.6)}$$

Where g is the gravitational constant (9.80665 m s^{-2}) and $d\theta/dz$ is the gradient of the potential temperature. For neutral or unstable conditions, ($d\theta/dz$ is zero or negative) the Brunt-Vaisala frequency is set equal to zero, and T_L is calculated using $\lambda = \lambda_n$. A consequence of Eq. (S5.2) and (S5.3) is, that the dispersion parameters for the plume segment dispersion are proportional to t for short travel time and proportional to $\sqrt{t}$ for long travel time.

The ground level concentration contribution $C_{point,p}$ from the plume segment released from a specific point source p to a certain receptor point is calculated using the Gaussian plume dispersion equation:

$$C_{point,p} = \frac{Q_p \cdot e^{-\lambda_w T_{add}}}{2\pi \cdot \mathrm{u} \cdot \sigma_y \cdot \sigma_z} \cdot \exp\left[-\frac{y_r^2}{2\sigma_y^2}\right] \cdot \left\{\exp\left[-\frac{(z_r - H_{eff})^2}{2\sigma_z^2}\right] + \alpha_p \cdot \exp\left[-\frac{(z_r + H_{eff})^2}{2\sigma_z^2}\right]\right\} \quad \text{(S5.7)}$$

where

x_r, y_r, z_r : receptor point location (x-axis is parallel with the wind direction),

Q_p : emission rate (g s^{-1}) for the point source, corresponding to the plume segment,

H_{eff} : effective emission height (m),

α_p : partial reflection coefficient due to dry deposition,

λ_w : wet scavenging coefficient (s^{-1}),

T_{add} : advection time from start of the plume segment to the receptor point (s).

Dry deposition from plume segments is calculated using the partial reflection approach (Hanna et al., 1982). Wet deposition is calculated using predefined scavenging rates and the (grid-cell average) precipitation rate. When the plume segment reaches a predefined horizontal or vertical extent or when the segmented plume experiences a large change in wind direction (larger than the redirection limit), it is inserted into the (Eulerian) main grid cell containing its centre of mass. The size of the critical extent is optimally set as $\frac{\sigma_y}{4} = 4$ or $\frac{\sigma_z}{4} = 4$, where σ_y and σ_z are the horizontal and vertical length scales of the plume segment, and Δy and Δz are the grid spacing in the

horizontal and vertical direction, respectively. Once the plume segment is transported outside of the model domain, its mass is lost. The model user can define (1) the maximum horizontal size (as grid cell fraction, default: 0.25) of the plume segments in each vertical model layer, (2) the redirection limit angle (default: 30°), and (3) the minimum wind speed (default: 0.4 m s^{-1}) in SEGPLU.

S6. Plume puffs (INPUFF)

The Gaussian puff model INPUFF (Petersen and Lavdas, 1986) calculates and keeps track of individual puffs and their pollutant concentrations as each is being released from a point source. Like the SEGPLU model, the INPUFF model handles the emission from specific point sources as a temporal sequence of instantaneous releases of a specified pollutant mass. The individual puffs are emitted at discrete time intervals $\Delta t = 3600/2N$, where N is an integer value which depends on the meteorological conditions, becoming larger with increasing wind speed. Unlike the SEGPLU model, the puffs in INPUFF are horizontally circular and can freely move with the wind flow even if the wind direction should abruptly change from one grid cell to the next, or from one hour to the next.

The initial horizontal position of the puff corresponds to the (x, y)-coordinates of the point source and the initial vertical position is estimated from plume rise formulas, where the plume rise is determined by stack height, stack exit velocity of the emitted pollutant and buoyancy of the effluent. Each puff is assumed to have a Gaussian concentration distribution horizontally (in both x- and y-direction) and also vertically with one primary source and one mirror source. The "size" of each puff is defined by the σ_x-, σ_y- and σ_z-values of the Gaussian distributions. The INPUFF model assumes that $\sigma_x = \sigma_y = \sigma_r$, i.e. that the puffs always remain horizontally circular throughout their lifetime. Initially, σ_r and σ_z are set equal to the diameter of the stack.

The puff starts to move in the direction of the wind at the point source at the final plume rise height. The mass of a pollutant in the puff is calculated as $M_{\text{puff},i} = Q_{p,i}\Delta t$ where $Q_{p,i}$ is the emission rate

of the point source. After release, the puffs are transported by horizontal advection, which for each time step is calculated as

$$X_{\text{puff}}\left(t+\Delta t\right)=X_{\text{puff}}\left(t\right)+u\Delta t$$
$$Y_{\text{puff}}\left(t+\Delta t\right)=Y_{\text{puff}}\left(t\right)+v\Delta t \qquad \text{(S6.1)}$$

Three dispersion schemes are incorporated in the model to account for initial, short travel time and long travel time dispersion. The initial dispersion scheme determines the size of the puff initially. After the puff is emitted from the source its growth is determined by one of two short travel time dispersion schemes: The Pasquill-Gifford (P-G) scheme which characterizes dispersion as a function of downwind distance; and an alternative scheme due to Irwin (1983) characterizing dispersion as a function of travel time. For long travel time, a scheme that enables the puff to grow as a function of the square root of time is used.

For details of the initial dispersion scheme in INPUFF (which includes processes of stack downwash and buoyancy), see Petersen and Lavdas (1986).

For short travel time, i.e. growth of σ_r up to 1000 m, dispersion is calculated using either the P-G scheme or the Irwin scheme. For the P-G scheme, P-G stability classes are used as inputs to the model. Further, P-G values applicable to areas characterized as rural are used. Two dispersion curves as given by Pasquill (1961) are incorporated in the model under neutral atmospheric conditions, namely curves D1 (D-day) and D2 (D-night) suitable for adiabatic and sub adiabatic conditions, respectively. The sigma-curves in the P-G scheme is based on data of close-to-ground level releases and short-distance dispersion studies. These data are used to continue the curves to greater release heights and larger source-receptor distances.

However, INPUFF is also capable of using actual meteorological data to estimate dispersion. Irwin (1983) proposed formulae for σ_y and σ_z following Cramer (1976) and Draxler (1976). According to this scheme, the crosswind and vertical dispersion of each puff are calculated as a function of travel time using

$$\sigma_y(t) = \sigma_v \cdot t \Big/ \left(1 + 0.9\sqrt{t/1000}\right) \tag{S6.2a}$$

and

$$\sigma_z(t) = \begin{cases} \sigma_w \cdot t & \text{for unstable conditions} \\ \sigma_w \cdot t \Big/ \left(1 + 0.9\sqrt{t/50}\right) & \text{for stable conditions,} \end{cases} \tag{S6.2b}$$

where σ_v and σ_w are the standard deviations of the horizontal crosswind and vertical wind fluctuations, respectively. Besides the P-G stability class, it requires σ_v and σ_w at the final plume height. Like for SEGPLU, σ_v and σ_w are calculated at this height in INPUFF using the profile method (Slørdal et al., 2003; Section 2.1).

A consequence of Eq. (S6.2a) and (S6.2b) is that the dispersion parameters for the puffs are proportional to t for short travel time and $\sqrt{t}$ for long travel time. INPUFF also incorporates a specific long-travel time scheme when σ_r becomes larger than 1000 m. For details of this scheme, see Petersen and Lavdas (1986).

The ground level concentration contribution $C_{\text{point},p}$ from a puff released from a specific point source p to a certain receptor point r is calculated using the Gaussian puff dispersion equation for horizontally circular puffs

$$C_{\text{point},p} = \frac{Q_p}{(2\pi)^{3/2}\sigma_r^2\sigma_z}\exp\left[-\frac{r^2}{2\sigma_r^2}\right]\left\{\exp\left[-\frac{(z_r - H_{\text{eff}})^2}{2\sigma_z^2}\right] + \exp\left[-\frac{(z_r + H_{\text{eff}})^2}{2\sigma_z^2}\right]\right\}, \quad \text{(S6.3a)}$$

where

r : horizontal distance from the puff centre to the receptor point (m),

z_r : height of the receptor point above ground (m),

H_{eff} : effective emission height (m),

Q_p : emission rate (g s^{-1}) for the point source, corresponding to the plume segment.

When σ_z becomes larger than 80% of the mixing height, H_{mix}, the puff is assumed to be vertically well- mixed and the concentration equation is then expressed as

$$C_{\text{point},p} = \frac{Q_p}{2\pi\sigma_r^2 H_{\text{mix}}}\exp\left[-\frac{r^2}{2\sigma_r^2}\right]. \quad \text{(S6.3b)}$$

Depending on the stack height, plume rise and mixing height, the puffs can be either above or below the height of the mixing layer and this will influence their growth rate. If a puff is above the mixing height it will grow according to the F-curve of the P-G scheme, or if Irwin's scheme is used, it's vertical growth will be characterized by $\sigma_w = 0.01$ ms^{-1}. After the puff attains a given size of σ_r specified by the user, its further growth will be proportional to $\sqrt{t}$. If a puff is below the mixing height its growth will depend on whether it is well-mixed vertically or not and whether its growth is according to t or $\sqrt{t}$. More details of this part of the model are given in Petersen and Lavdas (1986).

When two consecutive puffs are closer than a prescribed fraction of their sizes (as measured by σ_y of the younger puff) the puffs are merged together. The newly merged puff will receive parameters (position, travel time etc.) based on the mass-weighted average of the two puffs, except for the puff sigma values which is calculated according to the mass-weighted geometrical mean. The merged puff mass will be the sum of the two masses. Once the puff is transported outside of the model domain, the puff will be removed and not considered any further by the computation scheme.

For more details of the INPUFF model, see Petersen and Lavdas (1986).

S7. AROME Model Output Variables Used in EPISODE

Table S7.1 gives a list of the meteorological variables and other parameters from the AROME model (Denby and Süld, 2015) that are used in the EPISODE to calculate model the dynamics.

Table S7.1: Meteorological and model variables read in by EPISODE from the AROME netcdf files to calculate the model dynamics.

AROME Model variable	Units	Dimensions
Air temperature	K	3D
Pressure	Pa	3D
Specific humidity	kg m^{-3}	3D
Boundary layer height	m	2D
Downward eastward momentum flux in air	N m^{-2}	3D
Downward northward momentum flux in air	N m^{-2}	3D
Surface upward latent heat flux	W m^{-2}	2D
Surface upward sensible heat flux	W m^{-2}	2D
Surface upward water vapour flux	kg m^{-2} s^{-1}	2D
Air temperature 0m / Skin temperature	K	2D
Zonal wind X direction	m s^{-1}	3D
Zonal wind Y direction	m s^{-1}	3D
Turbulent kinetic energy	kg m^{-2}	3D
Hourly accumulated precipitation	kg m^{-2}	2D
Relative humidity 2m	-	2D
Cloud area fraction	-	2D
Elevation	m	2D
Surface roughness	m	2D
Model layer height	m	2D

S8. Quantitative Comparison of Meteorological Variables During Drammen and Oslo Case Studies

We present a comparison between the simulated meteorological input and observed meteorology (temperature and wind speed) for the two case studies discussed in Sect. 4.2 for Oslo and Drammen. Figures S8.1 and S8.2 present the temperature and wind speed for the Blindern, Oslo site comparison for December 9th to 13th. The meteorological observations were downloaded from the Norwegian Climate Service Center (https://klimaservicesenter.no/observations/, last access: 11th June 2020).

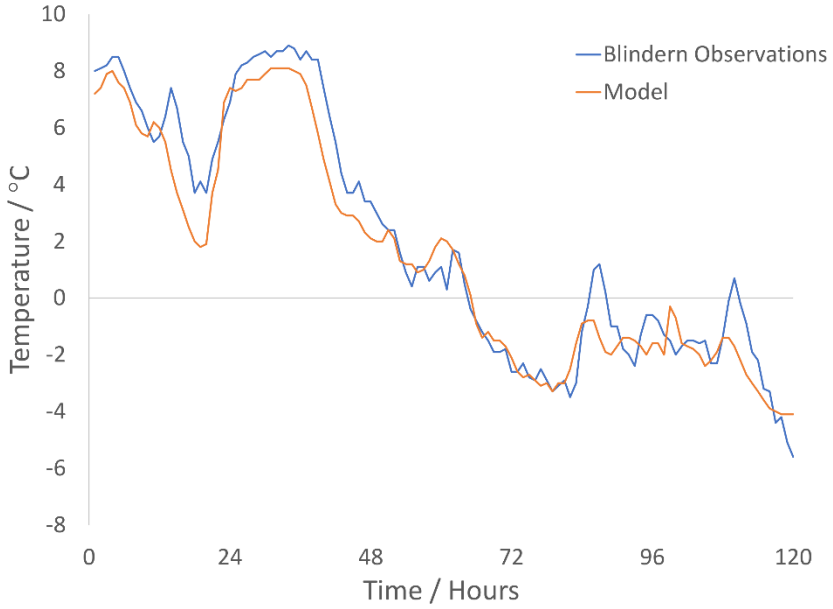

Figure S8.1: Time series of temperature in degrees Celsius for the Blindern meteorological station in Oslo during an NO_2 pollution episode lasting from December 9th to 13th. The blue line shows the observations and the orange line shows the meteorological input from AROME for the corresponding grid square over Blindern.

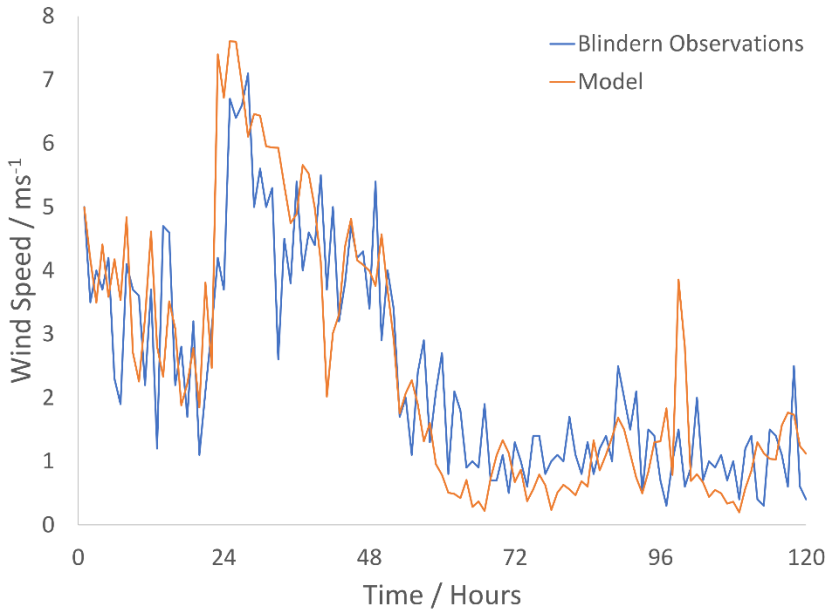

Figure S8.2: Time series of temperature in ms^{-1} for the Blindern meteorological station in Oslo during an NO_2 pollution episode lasting from December 9th to 13th. The blue line shows the observations and the orange line shows the meteorological input from AROME for the corresponding grid square over Blindern.

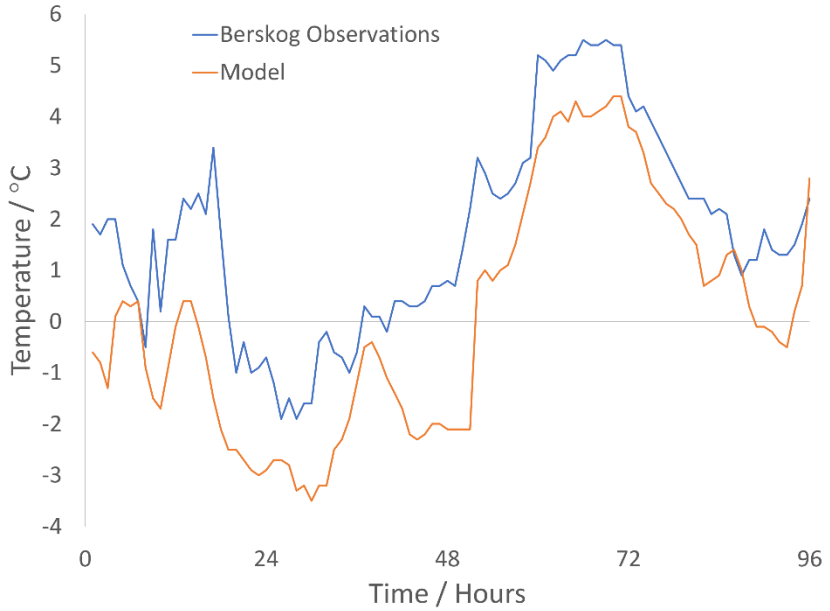

Figure S8.3: Time series of temperature in degrees Celsius for the Berskog meteorological station in Drammen during an NO_2 pollution episode lasting from January 4th to 7th 2015. The blue line shows the observations and the orange line shows the meteorological input from AROME for the corresponding grid square over Berskog.

Figures S8.3 and S8.4 present the temperature and wind speed for the Berskog, Drammen site comparison for January 4th to 7th.

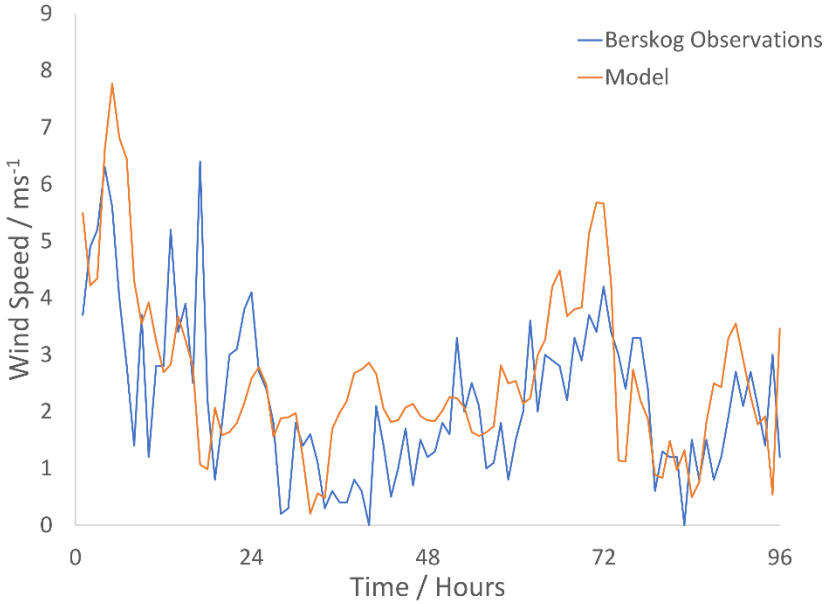

Figure S8.4: Time series of wind speed in ms^{-1} for the Berskog meteorological station in Drammen during an NO_2 pollution episode lasting from January 4th to 7th 2015. The blue line shows the observations and the orange line shows the meteorological input from AROME for the corresponding grid square over Berskog.

References

Briggs, G. A.: Plume Rise, US Atomic Energy Commission, Springfield, USA, 1–81, 1969.

Briggs, G. A.: Some recent analyses of plume rise observation, in: Proceedings of the Second International Clean Air Congress, edited by: Englund, H. M. and Berry, W. T., Academic Press, Washington, USA, 6–11 December 1970, 1029–1032, 1971.

Briggs, G. A.: Diffusion estimation for small emissions, Environmental research laboratories air resources atmospheric turbulence and diffusion laboratory 1973 annual report, USAEC Rep ATDL-106 Natl. Oceanic Atmos. Admin., Washington, DC, 1974.

Briggs, G. A.: Plume rise predictions, in: Lectures on Air Pollution and Environmental Impact Analysis, edited by: Haugen, D. A., Amer. Meteor. Soc., Boston, MA, pp. 59–111, 1975.

Byun, D. W., Young, J., Pleim, J., Odman, M. T., and Alapaty, K.: Chapter 7 "Numerical Transport Algorithms for the Community Multiscale Air Quality (CMAQ) Chemical Transport Model in Generalized Coordinates" In: Science Algorithms of the EPA Models-3 Community Multiscale Air Quality (CMAQ) Modeling System. EPA/600/R-99/030, U.S. Environmental Protection Agency, Office of Research and Development, Washington, DC, 1999.

Cramer, H.E.: Improved Techniques for Modelling the Dispersion of Tall Stack Plume. In: Proceedings of the Seventh International Technical Meeting on Air Pollution Modeling and its Application. NATO/CCMS, No. 51, pp. 731-780, 1976.

Denby, B. R. and Süld, J. K.: METreport NBV report on meteorological data for 2015 METreport, (January 2010), 2015.

Draxler, R.R.: Determination of Atmospheric Diffusion Parameters. Atmos. Environ., 10, 99-105, 1976.

Hanna, S. R., Briggs, G. A., and Hosker Jr., R. P.: Handbook on Atmospheric Diffusion, edited by: Smith, J. S., DOE/TIC-11223, Technical Information Center, US Department of Energy, Springfield, USA, 1982.

Holtslag, A. A., de Bruin, E. I. F., and Pan, H.-L.: A high resolution air mass transformation model for short-range weather forecasting, Mon. Weather Rev., 118, 1561–1575, 1990.

Holtslag, A. A. M. and de Bruin, H. A. R.: Applied modelling of the nighttime surface energy balance over land, J. Appl. Meteorol., 27(6), 689–704, 1998.

Irwin, J. S.: Estimating plume dispersion - a comparison of several sigma schemes. J. Clim. Appl. Meteor., 22, 92–114, 1983.

Karl, M., Castell, N., Simpson, D., Solberg, S., Starrfelt, J., Svendby, T., Walker, S.-E., and Wright, R. F.: Uncertainties in assessing the environmental impact of amine emissions from a CO_2 capture plant, Atmos. Chem. Phys., 14, 8533–8557, https://doi.org/10.5194/acp-14-8533-2014, 2014.

Pasquill, F.: The Estimation of the Dispersion of Wind-borne material. Meteorol. Magazine, 90, 33-49, 1961.

Petersen, W. B.: User's Guide for Hiway-2: A Highway Air Pollution Model, US Environmental Protection Agency, EPA-600/8-80-018, Research Triangle Park, NC, USA, 1980.

Petersen, W.B. and Lavdas, L.G.: INPUFF 2.0 – A Multiple Source Gaussian Puff Dispersion Algorithm. User's Guide. Research Triangle Park, NC., U.S. Environmental Protection Agency (EPA-600/8-86-024), 1986.

Slørdal, L. H., Solberg, S., and Walker, S. E.: The Urban Air Dispersion Model EPISODE applied in AirQUIS2003, Technical description, Norwegian Institute for Air Research, NILU TR 12/2003, Kjeller, Norway, 2003.

Venkatram, A., Strimaitis, D. and Dicristofaro, D.: A semiempirical model to estimate vertical dispersion of elevated releases in the stable boundary layer. Atmos. Environ. (1967), 18(5), 923–928, 1984.

Weil, J. C. and Brower, R. P.: An updated Gaussian plume model for tall stacks. J. Air Poll. Contr. Assess., 34, 818–827, 1984.

Walker, S. E. and Grønskei, K.E.: Spredningsberegninger for on-line overvakning i Grenland. Programbeskrivelse og brukerveiledning (In Norwegian), Norwegian Institute for Air Research, NILU OR 55/92, Kjeller, Norway, 1992.